Thermodynamics of Piperazine/Methyldiethanolamine/Water/Carbon Dioxide

Sanjay Bishnoi[†] and Gary T. Rochelle*

The University of Texas at Austin, Department of Chemical Engineering, Austin, Texas 78712

Vapor−liquid equilibrium, speciation, and amine solubility were studied for the piperazine (PZ)/methyldiethanolamine (MDEA)/water/carbon dioxide system. Solubility data for carbon dioxide in these solutions were obtained using a wetted-wall contactor. Solubility data for anhydrous PZ solid in water were obtained by adding PZ flakes to an agitated flask. In a 0.6 M PZ/4 M MDEA solution at 313 K, the partial pressure of carbon dioxide approaches one-tenth of the value in 4 M MDEA at low loading. This performance is between that of monoethanolamine (MEA) blends and diethanolamine (DEA) blends. The solubility data are modeled using the electrolyte NRTL model. The model is verified using ^{13}C and ^{1}H NMR data at high loading. The resulting model shows that the piperazine carbamate is the major reaction product at low loading (<0.1) while the protonated piperazine carbamate is the major reaction product at high loading. The piperazine dicarbamate species is present in higher concentration than in the simple PZ/H_2O/CO_2 system. Comparison to other blends (MEA/MDEA and DEA/MDEA) show that the dicarbamate and protonated carbamate species have a negative effect on the solubility of CO_2 at moderate loading. Amine volatility predictions are made using the Dortmund modification of the UNIFAC model to predict the activity coefficient of PZ in aqueous solutions. PZ volatility is very high; this model predicts PZ losses of the same magnitude as MDEA in a blend indicative of industrial concentrations, even though MDEA is present at much higher concentrations.

Introduction

Thermodynamics of aqueous amine systems are crucial to understanding their industrial use to remove acid gas from process gas streams. The equilibrium partial pressure of acid gas above a solution of the amine defines pinch conditions for the absorber and stripper. Speciation of the amine and reaction products defines the driving force for the forward and reverse reactions with CO_2. An understanding of this is important because the reactions are usually rate-controlling. Furthermore, a consistent thermodynamic model can quantify the energy required for regenerating the solvent and solvent losses due to amine volatility. This work studies piperazine (PZ)/methyldiethanolamine (MDEA)/H_2O solvents that have been applied to synthesis gas and natural gas.[1] Piperazine, $C_4H_{10}N_2$, is a symmetric diamine in a six-membered saturated ring.

Blended amine solvents have been studied by several researchers. Austgen et al.[2] studied the thermodynamics of MDEA blends with monoethanolamine (MEA), diethanolamine (DEA), and diglycolamine (DGA) using the electrolyte NRTL (nonrandom two liquid) model. Posey[3] improved the models by studying the activity coefficient of the amines at infinite dilution. Pacheco et al.[4] studied the absorption of CO_2 into aqueous DGA/MDEA blends. Glasscock et al.[5] and Critchfield[6] have studied blends of DEA and MEA/MDEA. Littel et al.[7] and Rinker et al.[8] have studied a variety of tertiary amines promoted by primary or secondary amines. The rate constant of PZ has been found to be a factor of 10 higher than that of conventional alkanolamines such as MEA.[9] This paper will demonstrate that the high rate of reaction, and not the thermodynamics, is the major reason PZ blends have a higher mass-transfer capability than many other blends studied.

Specifically, this work will use the thermodynamic frameworks presented by Bishnoi and Rochelle,[10] Austgen et al.,[2] and Posey and Rochelle.[11] Data acquired by Xu et al.[12] and Liu et al.[13] for the PZ/MDEA system at high loading will also be discussed. Insight into the interaction of PZ with CO_2 discussed by Bishnoi and Rochelle[9] will also be useful in setting up the chemistry framework of the model.

The simple system of PZ/H_2O is represented by estimating the infinite dilution activity coefficient of PZ using the Dortmund modification of the UNIFAC model.[14] The solubility limit of PZ was measured. A wetted-wall column was used to measure CO_2 solubility at conditions where the ratio of total carbon dioxide to PZ is less than 1. Parameters of the electrolyte NRTL model were adjusted in order to match the CO_2 solubility data at low loading and the NMR data at high loading.

Experimental Methods

Solubility of carbon dioxide was determined using a wetted-wall apparatus. The use of this apparatus to extract data for CO_2 solubility in amine solutions has been described by Bishnoi and Rochelle.[9] Absorption and desorption data are bracketed, and flux is interpolated to zero to determine the equilibrium solubility partial pressure of CO_2 at a given solution loading. Samples of the liquid demonstrate that the loading has not changed during the absorption and desorption events.

A round-bottom flask was used to mix solid PZ and water and measure the solubility of PZ in H_2O. The flask was agitated from above, and temperature was controlled using a Lauda heater and water bath. Anhydrous PZ solid was added until the solubility limit was achieved. The agitator was shut off, and the solution was allowed to settle before liquid samples were with-

* Author to whom correspondence should be addressed. Phone: 512-471-7230. Fax: 512-475-7824. E-mail: rochelle@che.utexas.edu.

[†] Current address: The Boston Consulting Group, Dallas, TX.

10.1021/ie0103106 CCC: $22.00
Published on Web 01/03/2002

Table 1. Activity Coefficients at Infinite Dilution in Water at 25 °C

species	infinite dilution activity coefficient	source
PZ	0.24	Dortmund-modified UNIFAC
piperidine	5.6[a]	Dortmund database
amino-ethane	0.53[b]	Dortmund database
hexylamine	29	Dortmund database
hexane	871[b]	Dortmund database
PZ (in 4.28 M MDEA)	0.11	Dortmund-modified UNIFAC

[a] Extrapolated from data at 70−100 °C. [b] Interpolated from data at 20 and 30 °C

drawn off the top of the flask and titrated with 2 N HCl to an endpoint pH of 2 to determine the total PZ content. The sampling technique was tested by performing the experiment at ambient temperature and filtering the solid/liquid mixture. The sampling technique gave the same result as the filtered experiment.

NMR experiments were performed at 25 °C on a Varian EM-390. ^{13}C, ^{1}H, and C−H short-range correlation NMR spectra were measured using D_2O solvent.

Activity of Piperazine in Aqueous Mixtures. Table 1 presents the activity coefficients at infinite dilution predicted by the Dortmund modification of the UNIFAC theory.[14] All of the parameters necessary for calculation of the activity coefficients are given in the paper by Gmehling et al.[14] The value obtained for the PZ activity coefficient matches that of similar molecules measured at 25 °C. Table 1 shows a comparison of measured activity coefficients at infinite dilution and 25 °C. The comparison of hexane with hexylamine demonstrates that the addition of a nitrogen to a hydrocarbon significantly reduces its activity coefficient. The comparison of piperidine to hexylamine demonstrates that a cyclic secondary amine has a lower activity coefficient than a comparable noncyclic primary amine. Piperidine is also very similar to PZ in that it is a six-membered ring. To convert piperidine to PZ, we would remove one hydrophobic methylene group and add a hydrophilic amine group. This would decrease the activity coefficient to a value less than that of piperidine (<5.6). The calculated value of 0.24 using the Dortmund-modified UNIFAC model reported in this work is consistent with this trend. Furthermore, amino-ethane has the same ratio of methylene groups to amine groups. Amino-ethane is, in fact, half a PZ molecule. The experimental value of 0.53 for amino-ethane qualitatively compares well with the estimated PZ value.

Table 1 also shows the behavior of the PZ activity coefficient in the presence of MDEA. The model predictions of UNIFAC suggest that the activity of PZ decreases as MDEA is added to the system.

Wilson and Wilding[15] have measured vapor−liquid equilibrium for the PZ/H_2O system at elevated temperatures. Examination of their data at 112.9 and 198.8 °C yields activity coefficients of 0.15 and 1.0, respectively, for PZ at infinite dilution in H_2O. Analysis of activity coefficients at the two temperatures they studied and eq 1 yields an excess heat of mixing at infinite dilution of −37.7 kJ/mol for liquid PZ.

$$\ln\left(\frac{\gamma_{PZ}^{(2)}}{\gamma_{PZ}^{(1)}}\right)_{P,x} = \frac{h_2^{Ex}}{R}\left[\frac{1}{T^{(2)}} - \frac{1}{T^{(1)}}\right] \qquad (1)$$

Table 2. Excess Heat of Mixing at Infinite Dilution and 25 °C

species[a]	$h_{AM}^{Ex,\infty}$ (kJ/mol)	source
piperazine	−59	Dortmund-modified UNIFAC[b]
piperazine	−38	Wilson and Wilding[15]
piperidine	−26	Dohnal et al.[30]
morpholine	−25	Dohnal et al.[30]
cyclohexylamine	−23	Dohnal et al.[30]

[a] All species listed are liquids in their pure state at ambient conditions except PZ. [b] Reference state of most components in Dortmund UNIFAC database is liquid.

Table 3. Solubility Limit of Piperazine in H_2O

	PZ solubility			PZ solubility	
T (K)	(M)	mole fraction	T (K)	(M)	mole fraction
273	0.52	9.7×10^{-3}	323	7.83	0.323
294	1.64	3.3×10^{-2}	333	8.17	0.376
298	1.88	3.4×10^{-2}	343	8.40	0.414
313	7.42	0.270			

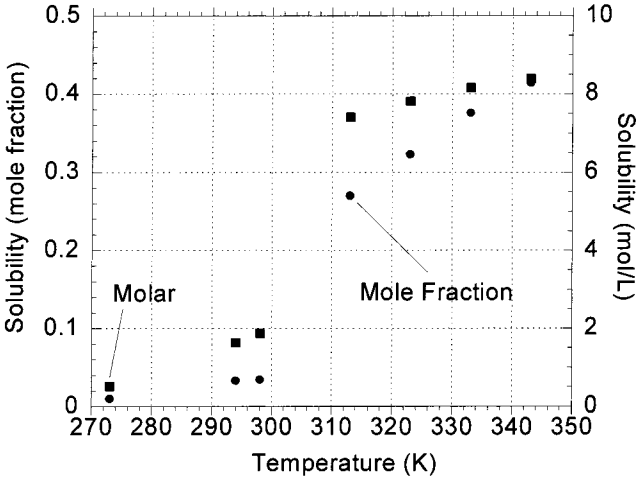

Figure 1. Solubility of anhydrous PZ solid in H_2O.

A comparison of values of the excess heat of mixing at infinite dilution is provided in Table 2. The value for amines is consistently negative and seems to be related to the amino group. The value (−59) calculated by the Dortmund modification of UNIFAC is about twice the measured value of piperidine, butylamine, and morpholine. This is reasonable because piperazine has two amine functions.

In this work, NRTL parameters for PZ/H_2O and H_2O/PZ have been fit to values of the activity coefficient at infinite dilution calculated by the Dortmund-modified UNIFAC model. These parameters are reported later in Table 6. Accurate prediction of the PZ activity coefficient helps predict PZ volatility and losses as well as correcting the equilibria that involve PZ for the effect of MDEA.

Solubility of Piperazine in Water. The initial concentration of PZ in the solvent is limited on the higher end by its solubility in water and MDEA solutions. This solubility limit was measured using the apparatus discussed previously, and the results are presented in Table 3 and Figure 1. Below 40 °C (313 K) the solubility is limited by formation of the PZ hexahydrate which melts at 316 K.[16] The melting point of the hydrate explains the discontinuity at around 40 °C (313 K) in Table 3.

Table 4. Miscellaneous Constants for VLE Model and Temperature-Dependent Constants

(a) Miscellaneous Constants for VLE Model

constant	carbon dioxide	water	MDEA	piperazine
critical T (K)	304.2	647.3	677.79	638.0
critical P (kPa)	7376	22 090	3876	6870
critical V (m^3/mol)	9.4×10^{-2}	5.7×10^{-2}	0.39	0.23
accentric factor	0.23	0.34	1.24	0.80
rackett Z_{RA}	0.27	0.24	0.19	0.20
Brelvi−O'Connell	9.6×10^{-2}			

(b) Temperature -Dependent Constants (K)

	a	b	c	d	e
Henry's Law constant (Pa/mole fraction)	$\ln H_x = a + b/T + c \ln T + dT$				
carbon dioxide	170.71	−8477.7	−21.95	0.005 781	
dielectric constant	$De = a + b[1/T - 1/273.15]$				
H_2O	88.36	33 030			
MDEA	24.76	8 989			
PZ	36.76	14 836			
Antoine equation (Pa)	$\ln P^{SAT} = a + b/T + c \ln T + dT^e$				
H_2O	72.55	−7206.7	−7.1385	4.04×10^{-6}	2.0
MDEA	26.137	−7588.5	0.0	0.0	0
PZ	172.78	−13 492	−21.91	1.378×10^{-5}	2.0

Model Description

A flexible Fortran code for the solution and phase equilibrium of acid gas systems was developed by Austgen.[17] This code was modified slightly to model PZ-activated MDEA blends. The model uses the Smith and Missen[18] nonstoichiometric algorithm to speciate the liquid solution. Equilibrium constants were used to calculate the standard-state chemical potentials using the method described by Austgen.[17] The following reactions and species are considered. All of the PZ species shown have been shown to exist in aqueous PZ solutions loaded with CO_2 by Bishnoi and Rochelle.[9]

$$CO_2(aq) + 2H_2O \leftrightarrow HCO_3^- + H_3O^+ \quad (2)$$

$$HCO_3^- + H_2O \leftrightarrow CO_3^{2-} + H_3O^+ \quad (3)$$

$$2H_2O \leftrightarrow H_3O^+ + OH^- \quad (4)$$

$$PZH^+ + H_2O \leftrightarrow PZ + H_3O^+ \quad (5)$$

$$PZ + CO_2 + H_2O \leftrightarrow PZCOO^- + H_3O^+ \quad (6)$$

$$H_2O + H^+PZCOO^- \leftrightarrow H_3O^+ + PZCOO^- \quad (7)$$

$$PZCOO^- + CO_2 + H_2O \leftrightarrow {}^-OOCPZCOO^- + H_3O^+ \quad (8)$$

$$MDEAH^+ + H_2O \leftrightarrow MDEA + H_3O^+ \quad (9)$$

The total amount of water, carbon dioxide, PZ, and MDEA present in the liquid phase are specified. Equilibrium is first calculated in the liquid phase, and then vapor−liquid equilibrium is calculated for all molecular species (PZ, MDEA, H_2O, CO_2).

Gas-phase nonidealities are calculated using the SRK equation of state.[19] Liquid-phase nonidealities are calculated using the electrolyte NRTL model.[20−22] The use of the electrolyte NRTL model in amine/acid gas systems has been described previously by Austgen et al.,[2] Posey,[3] and Bishnoi and Rochelle.[10] This work most closely resembles that of Bishnoi and Rochelle[10] with CO_2 referenced to infinite dilution in water. All ions are also referenced to infinite dilution in water. PZ, MDEA, and H_2O are all referenced to the respective pure components at the system temperature (i.e., pure anhydrous PZ solid).

Protonated PZ carbamate (H^+PZCOO^-) is defined as an anion with no net charge. As a result, its activity coefficient does not deviate significantly from unity. Identifying this species as an anion, even though it does not have net charge, avoids dealing with its volatility. It is assumed that this species is nonvolatile.

The parameters for molecule−molecule interactions, τ_i, are defined to be consistent with the work of Bishnoi and Rochelle[10]

$$\tau = A + \frac{B}{T} \quad (10)$$

Values of interaction parameters for salt pair/molecule and molecule/salt pair are defined as

$$\tau = A + B\left(\frac{1}{T} - \frac{1}{T_{ave}}\right) \quad (11)$$

Here, T is temperature in kelvin and T_{ave} is 353.15 K.

Default parameters consistent with Aspen Plus version 8.5 were used in this work. This is consistent with the work of Austgen et al.,[2] Posey,[3] and Bishnoi and Rochelle.[10] A description of these defaults is as follows. All B parameters are 0. For A parameters, all molecule/molecule are 0, all water/salt pair are 8.0, all salt pair/water are −4, all molecule (other than water)/salt pair are 15, and all salt pair/molecule (other than water) are −8. All molecule/molecule, water/salt pair, and salt pair/water nonrandomness parameters are 0.2. All other nonrandomness parameters are 0.1.

Critical constants used by the SRK equation of state and the accentric factor were taken from the DIPPR database.[23] The Henry's law constant for CO_2 was fit by Chen et al.[24] Brelvi−O'Connell parameters used in this work were obtained from the original work of Brelvi and O'Connell.[25] Critical compressibilities used in the Rackett model were obtained from the DIPPR database. The dielectric constant of PZ was assumed to be the same as that of MEA. Although this is purely an assumption, the mole fraction of PZ is so small that it will have a negligible effect on the calculated results.

Table 5. Temperature Dependence of Equilibrium Constants, Mole Fraction-Based ln (K_x) = $A + B/T + C$ ln T, T (K)

eq no.	equilibrium constant	A	B	C	value at 313 K	source
2	$\frac{a_{HCO_3^-}a_{H_3O^+}}{a_{CO_2}a_{H_2O}^2}$	231.4	−12 092	−36.78	8.55×10^{-9}	Posey[3]
3	$\frac{a_{H_3O^+}a_{CO_3^=}}{a_{HCO_3^-}a_{H_2O}}$	216.0	−12 432	−35.48	1.04×10^{-12}	Posey[3]
4	$\frac{a_{H_3O^+}a_{OH^-}}{a_{H_2O}^2}$	132.9	−13 446	−22.48	9.15×10^{-18}	Posey[3]
5	$\frac{a_{PZ}a_{H_3O^+}}{a_{H_2O}a_{PZH^+}}$	4.964	−9 714.2	0.0	4.76×10^{-12}	Pagano[31]
6	$\frac{a_{H_3O^+}a_{PZCOO^-}}{a_{PZ}a_{CO_2}a_{H_2O}}$	−41.583	9 288.2	0.0	6.73×10^{-6}	this work
7	$\frac{a_{PZCOO^-}a_{H_3O^+}}{a_{H^+PZCOO^-}a_{H_2O}}$	−13.041	−3 961.6	0.0	6.91×10^{-12}	this work
8	$\frac{a_{H_3O^+}a_{^-OOCPZCOO^-}}{a_{PZCOO^-}a_{CO_2}a_{H_2O}}$	−44.7	9 288.2	0.0	2.98×10^{-7}	this work
9	$\frac{a_{MDEA}a_{H_3O^+}}{a_{MDEAH^+}a_{H_2O}}$	−9.4165	−4 234.98	0.0	1.09×10^{-10}	Posey[3]

The Antoine equation for PZ was obtained from Stephenson and Malanowski.[26] It is important to note that the vapor pressure of PZ below 106 °C refers to the sublimation pressure of anhydrous PZ. The Antoine equation in the DIPPR database is only valid above the triple point and would, therefore, incorrectly describe the sublimation of solid PZ below 106 °C. Values of all of these constants are documented in Table 4.

Parameter Regression Results. Equilibrium constants for reactions 2−9 are documented in Table 5 along with their sources. The first and second dissociation constants of CO_2, the MDEA protonation, and water dissociation constants are unchanged from the work of Austgen.[17] Constants for reactions 6−8 are based on the experimental work of Bishnoi and Rochelle.[9]

CO_2 solubility and NMR data were re-regressed to obtain equilibrium constants consistent with the aqueous PZ data and the reference state of this work. It should be noted here that all of the parameters involving PZ salts/water were kept at their default values in this work. All of the parameters involving MDEA salt pairs and water are the parameters regressed by Bishnoi and Rochelle.[10] The resulting model, therefore, matches data in aqueous PZ solutions as well as data in MDEA and MDEA/PZ solutions.

Values of all nondefault parameters are listed in Table 6 along with their default values and sources. Regression was performed using GREG.[27] The $CO_3^=$-MDEAH$^+$/MDEA A parameter was changed to 15 from its regressed value of 24.5 because the model would not converge with a value of 24.5. This parameter was seen to have a very large standard deviation;[3,10] therefore, changing it has had a very small effect on calculated partial pressure. More importantly, the model still matches data in aqueous MDEA.

$\tau_{PZ/MDEA}$ was also adjusted instead of using the value calculated by the UNIFAC model. It was found that only a very approximate fit of the CO_2 solubility data could be achieved unless this parameter was adjusted. The resulting activity coefficient for PZ predicted by the model at very low loading, 313 K and 4 M MDEA and 0.6 M PZ, is 0.09 as compared to 0.35 predicted by the UNIFAC model. The activity coefficient of PZ at infinite dilution in water is predicted by UNIFAC to be about 2 times greater than that in 4.3 M MDEA (Table 1). The shift in the activity coefficient from water to a concentrated MDEA solution, therefore, matches the UNIFAC model in direction but not quantitatively. The inability to match data without adjusting this parameter stresses its importance.

Table 6. Nondefault Parameters for the NRTL Model

parameter	A	B	τ_{40}	default τ
H_2O (C5 + HCO_3^-)	9.645	0	9.65	8
(C5 + HCO_3^-) H_2O	−4.483	652.4	−4.25	−4
(C5 + HCO_3^-) MDEA	−6.211	−3056.8	−7.32	−8
(C5 + $CO_3^=$) MDEA	15	0	15	−8
(C5 + OH^-) H_2O	−5.16	0	−5.16	−4
(C5 + HCO_3^-) CO_2	−8.08	2840.8	−7.05	−8
CO_2 MDEA	1.637	0	1.64	0
H_2O CO_2	0	0	0	0
CO_2 H_2O	0	0	0	0
H_2O MDEA[a]	9.473	−1902.4	3.40	0
MDEA H_2O[a]	−2.173	−147.4	−2.64	0
(PZH + $PZCOO^-$) MDEA	−7.305	−2625.5	−8.25	−8
PZ/MDEA	−12.182	2801.1	−3.23	0
($PZ(COO^-)_2MDEAH^+$) H_2O	−4.2	0	−4.2	−4

[a] Obtained by ref 3. $\tau = A + B[(1/T) - (1/353.15)]$ for salt pair/molecule and molecule/salt pair. $\tau = A + B/T$ for molecule/molecule.

The regressed τ value for PZH^+PZCOO^-/MDEA obtained in this work does not deviate far from the default value. The value for $PZ(COO^-)_2MDEAH^+/H_2O$ has been adjusted to match NMR data taken in 1 M PZ/3 M MDEA solutions loaded with carbon dioxide. Once this parameter was adjusted, the data for CO_2 solubility were regressed again to determine τ values for PZH^+-$PZCOO^-$/MDEA and PZ/MDEA. This was done several times until none of the parameters observed any significant changes from the previous iteration. The NMR data will be discussed further in a later section.

Solubility of Carbon Dioxide in Aqueous PZ/MDEA. Data for CO_2 solubility in PZ/MDEA/H_2O blends were obtained in this work. Data in 0.6 M PZ/4 M MDEA at 313 and 343 K and 4.28 M MDEA at 313 K are given in Table 7 and Figure 2. Throughout this work, loading is represented as mol of CO_2/mol of amine where the total molar concentration of amine is equal

Table 7. CO_2 Solubility in Piperazine-Activated MDEA

313 K				343 K	
4.28 M MDEA		0.6 M PZ, 4 M MDEA		0.6 M PZ, 4 M MDEA	
loading[a]	P_{CO_2}* (Pa)[b]	loading	P_{CO_2}* (Pa)	loading	P_{CO_2}* (Pa)
0.013	108	0.027	33	0.006	34
0.024	505	0.061	115	0.014	241
0.032	730	0.073	236	0.020	491
		0.089	367	0.046	780
		0.140	1140	0.093	3600
		0.140	1335		
		0.188	2550		
		0.285	7480		

[a] Estimated error in loading is ±5%. [b] Estimated error in partial pressure is ±30%.

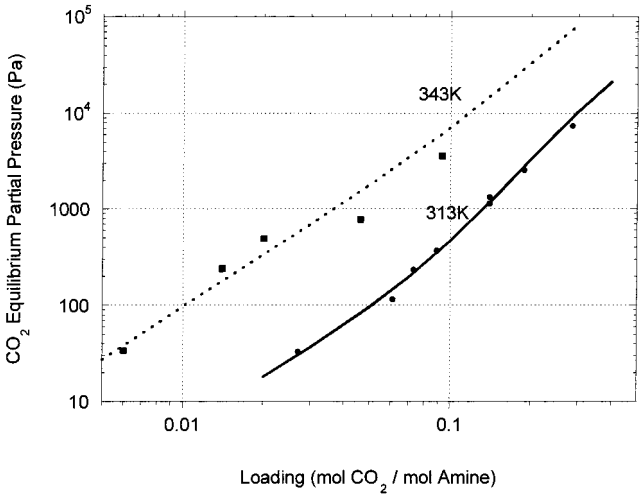

Figure 2. Measured and predicted solubility of CO_2 in 0.6 M PZ/4 M MDEA solutions.

to the molar concentration of MDEA plus the molar concentration of PZ.

The addition of roughly 5 wt % of PZ to a 45 wt % of aqueous MDEA solution reduces the equilibrium partial pressure of CO_2 by a factor of 10 at low loading. The data converges with the equilibrium partial pressure of MDEA at a CO_2 loading greater than 0.2. The model presented in this work matches data in aqueous PZ, MDEA and PZ/MDEA blends.

Xu et al.[12] obtained solubility data for CO_2 in solutions of 4.28 M MDEA and 0−0.5 M PZ solutions at 343 K. Their data is all taken at conditions where the ratio of total carbon dioxide to PZ is close to or greater than 1. The equilibrium partial pressure of CO_2 was not found to be significantly different than that in MDEA alone at those conditions. Their data, however, are very helpful in studying the high loading region because our experimental data were not acquired in this region.

In a further piece of work by the same research laboratory, Liu et al.[13] obtained a large amount of data in solutions of variable MDEA and PZ concentration. Again, most data taken complements the data taken in this work because it is at high loading with respect to PZ concentration. Our model is found to predict their data well, as shown by the parity plot in Figure 3. The data of Xu et al.[12] and Liu et al.[13] taken within the temperature range studied in this work has approximately the same standard deviation as our data. Although represented well by the model, the data taken outside the temperature range studied in this work (303 and 363 K) has a larger standard deviation. This may

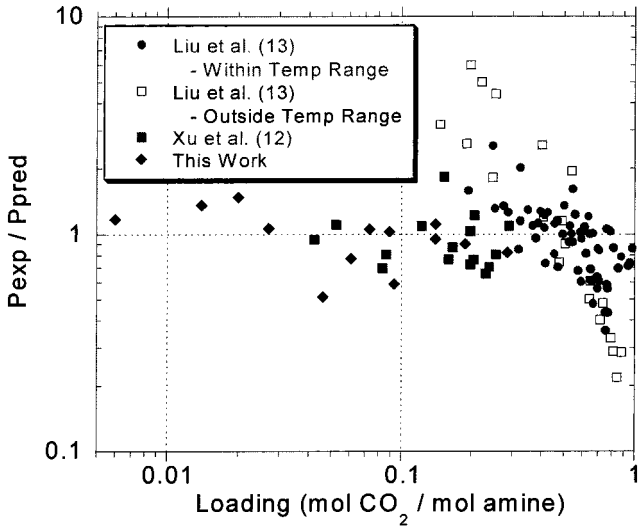

Figure 3. Model predictions for all CO_2 solubility data in PZ/MDEA blends.

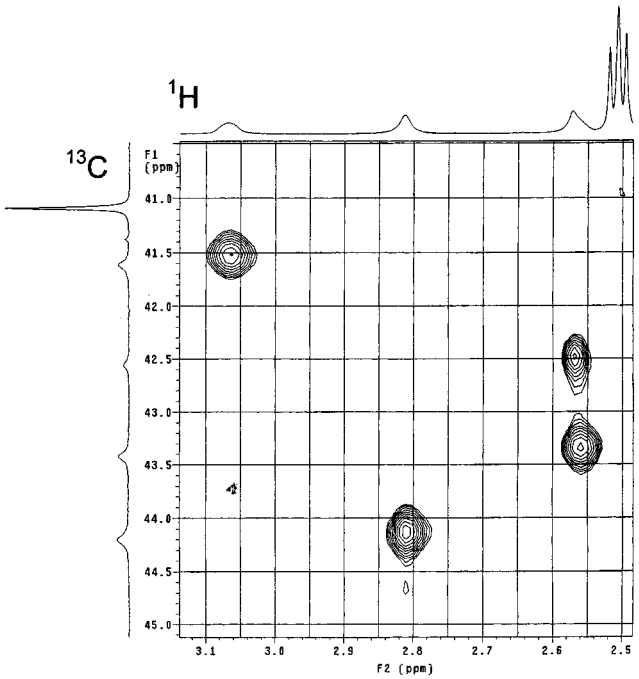

Figure 4. ^{1}H, ^{13}C, and short-range C−H correlation NMR spectra for a 1 M PZ/3 M MDEA solution at 298 K and 0.52 mol of CO_2/mol of amine.

be due to an erroneous temperature extrapolation of equilibrium constants or to activity coefficient parameters beyond the range of our data. A detailed list of all other data for CO_2 solubility in PZ/MDEA blends is shown in Appendix E of Bishnoi[28] along with the predictions of the model presented in this work.

Analysis of Xu et al.[12] data with MDEA alone shows that their data is increasingly lower in partial pressure than the data of other investigators[29] as loading is increased. This trend is consistent with the downward trend in data shown in Figure 3 for the PZ/MDEA data taken in the same equipment, leading us to believe that there may be some systematic error in the data.

No formal analysis or modeling of the PZ reactions was presented in the work of Xu et al.[12] The work of Liu et al.[13] considers only the protonation of PZ. They ignore the formation of the carbamate, dicarbamate, and protonated carbamate in their work. Because their data

Table 8. NMR Data for 0.6 M PZ/4 M MDEA at 298 K and 0.52 mol of CO_2/mol of Amine

^{1}H peak			^{13}C peak	
δ (ppm)	area	species	δ (ppm)	species
3.323	2.67	methylene H's adjacent to alcohol in MDEA	41.08	methyl C in MDEA
3.311			41.60	carbamate ring C's adjacent to carbamate side
3.300			42.55	
3.067	0.49	protonated carbamate/carbamate methylene H's on carbamate side	43.41	carbamate ring C's adjacent to non-carbamate side
2.812	0.62	methylene H's in piperazine dicarbamate	44.2	dicarbamate ring C's
2.571	0.73	protonated carbamate/carbamate methylene H's on non-carbamate side	58.69	methylene C's adjacent to alcohol in MDEA
2.517	2.67	PZ/protonated PZ methylene H's and methylene H's adjacent to amine in MDEA	57.78	methylene C's adjacent to amine in MDEA
2.505				
2.494				
2.136	2.00	MDEA methyl H's		

Table 9. Ratio of Species Using NMR Data at 298 K, 1 M PZ, 4 M MDEA, Loading = 0.52

ratio	NMR	calcd
$x_{PZ(COO^-)_2}/(x_{PZCOO^-} + x_{H^+PZCOO^-})$	0.63	0.63
$(x_{PZCOO^-} + x_{H^+PZCOO^-})/(x_{PZ} + x_{PZH^+})$	4.1	3.1
$x_{PZ(COO^-)_2}/(x_{MDEAH^+} + x_{MDEA})$	0.12	0.11

was taken at conditions where the equilibrium partial pressure of CO_2 is mainly dictated by MDEA, they were able to explain their data. No attempt was made to replicate their model and to run it at the conditions of our data.

NMR Data. ^{1}H, ^{13}C, and C−H correlation NMR experiments were performed on solutions of 1 M PZ/3 M MDEA and on CO_2-loaded solutions of 3 M MDEA and 1 M PZ/3 M MDEA. We were able to distinguish between PZ/protonated PZ, carbamate/protonated carbamate, dicarbamate, and MDEA/protonated MDEA with the NMR spectra. Figure 4 shows the ^{13}C−^{1}H NMR correlation spectra. Comparison of this spectrum to the spectrum presented by Bishnoi and Rochelle[9] for the PZ/D_2O/CO_2 system shows that the carbon peaks have not shifted significantly in the presence of MDEA solvent. The hydrogen peaks have shifted quite a bit. We are unable to see the triplets associated with the carbamate species.

This is most probably due to a faster transfer of the deuterium. The C−H correlation, however, confirms that the relative positions of the species have not shifted. Numerical placement of the peaks is shown in Table 8.

We can calculate the ratios of species present using the areas of the ^{1}H spectra. Table 9 shows the ratios of several PZ and MDEA species as measured by ^{1}H NMR data along with the calculated values at the same conditions. The ratio of dicarbamate to mono- and protonated carbamate was matched by adjusting the PZ-$(COO^-)_2$MDEAH$^+$/H_2O *A* parameter. Other predicted ratios match the experimentally observed values well.

Model Predictions. Figure 5 shows the calculated equilibrium partial pressure of CO_2 in 4 M MDEA with 0−0.6 M PZ at 313 and 343 K. The strongest effect of PZ is to reduce P_{CO_2} at low CO_2 loading. At moderate and high CO_2 loading, the effect of PZ is to slightly reduce P_{CO_2}. This is seen more clearly in Figure 6 which compares the ratio of equilibrium partial pressure in several promoted MDEA systems (0.5 M promoter, 4 M MDEA) to that of 4 M MDEA. The curves for MEA and DEA are those calculated by Austgen.[17] The ratio of

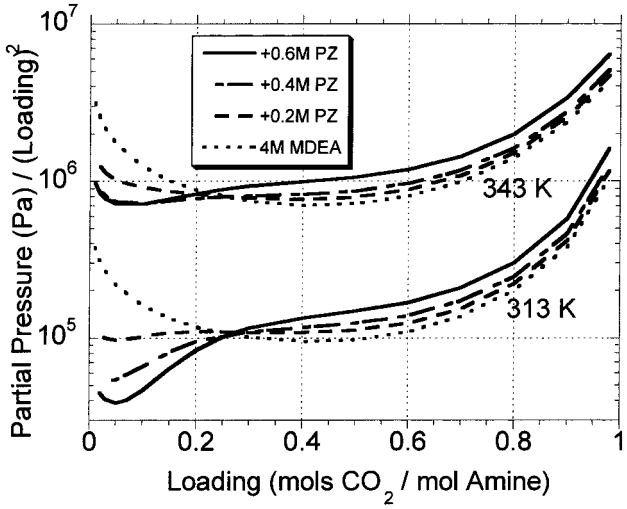

Figure 5. Equilibrium partial pressure predictions for CO_2 in 4 M MDEA and various PZ concentrations.

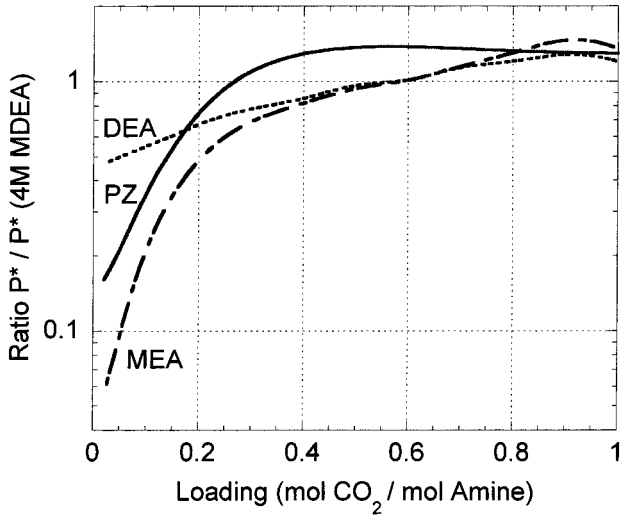

Figure 6. Comparison of PZ to other promoters in 0.5 M promoter/4 M MDEA.

partial pressures at a loading approaching 0 is determined exclusively by the carbamate stability constant. Table 10 includes values of the carbamate stability constants for these three amines using the reference states of this work. Because the carbamate stability of DEA and PZ are almost identical, it is not apparent at first that there is any correlation between the ratio of

Table 10. Comparison of Carbamate Stability Constants (313 K, Mole Fraction)[a]

amine	all species at their reference state	at infinite dilution in aqueous solution	in 4 M MDEA (at 0 loading)
DEA	4.8×10^{-6}	2.64×10^{-6}	2.5×10^{-7}
PZ	6.7×10^{-6}	1.1×10^{-5}	8.7×10^{-6}

[a] $K_{CARB} = (X_{RR'NCOO^-} X_{H_3O^+})/(X_{H_2O} X_{CO_2} X_{RR'NH})$.

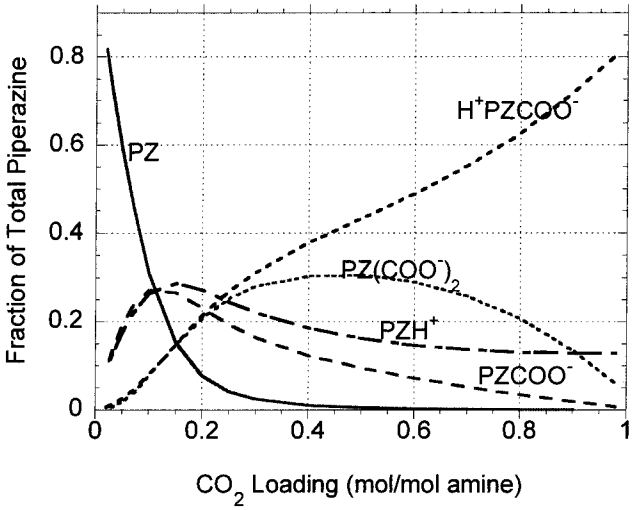

Figure 7. Speciation of 0.5 M PZ/4 M MDEA at 313 K. Results are shown as a fraction of total piperazine.

partial pressures at very low loading and the carbamate stability constant.

In the presence of 4 M MDEA, the activity coefficients of all PZ species are significantly different than those in water alone. Lumping the activity coefficients in the equilibrium constant so that it is expressed on a mole fraction basis, the correlation between carbamate stability and CO_2 solubility becomes more apparent. Table 10 presents the carbamate stability constant at different conditions. The carbamate stability constant of DEA and PZ differ substantially in 4 M MDEA, even though they are comparable when all species are at their reference states.

At higher loading, the partial pressure in promoted MDEA systems is often higher than that of MDEA systems. This is seen to be the case for MEA, DEA, and PZ in Figure 6. Austgen[17] presents a discussion on this phenomenon where he shows this to be related to the 2:1 stoichiometry of carbamate formation. In DEA and MEA blends, this crossover point occurs around a loading of 0.6. In the PZ system, however, we see the crossover at a much lower loading. This is because of the many different carbamate species that are formed, resulting in greater than a 2:1 stoichiometry for overall carbamate formation. Explained a different way, the presence of the protonated PZ carbamate and the PZ dicarbamate increase the overall stability of the carbamate species, resulting in more amine being tied up for every mole of carbon dioxide absorbed.

This can be observed by comparing the speciation of the PZ system to the DEA system. Figures 7 and 9 compare the speciation of the PZ and DEA blends at 313 K. The PZ concentration disappears almost completely by a loading of 0.2, and the concentration of PZ carbamate and protonated PZ seem to track each other, rising at low loading and reaching a maximum at a loading of 0.2. Conceptually, these trends exist in DEA as well, with the concentration of free DEA staying

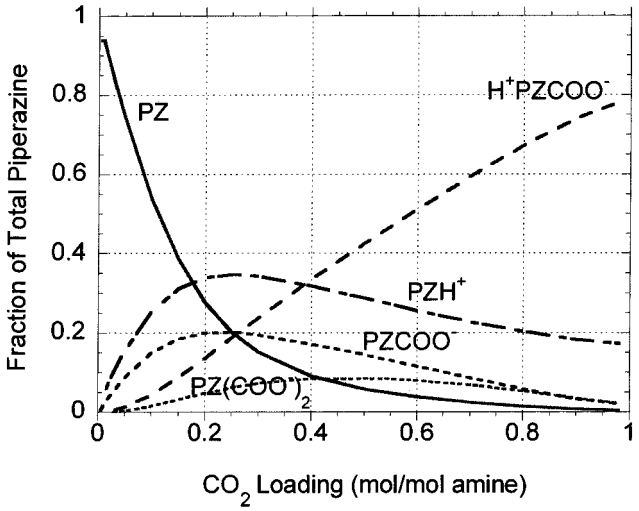

Figure 8. Speciation of 0.5 M PZ/4 M MDEA at 343 K. Results are shown as a fraction of total piperazine.

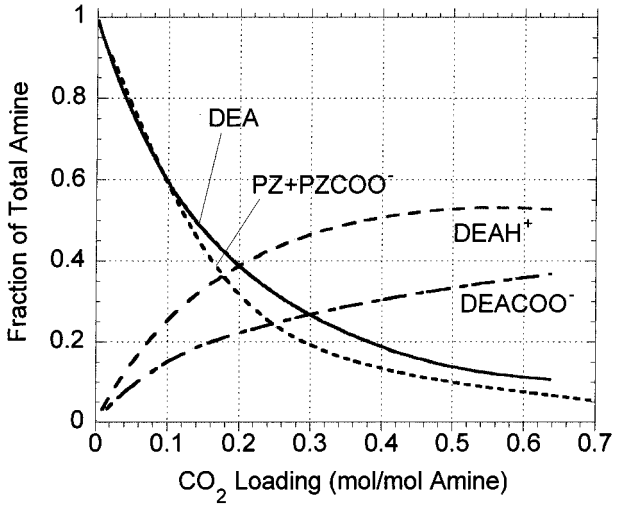

Figure 9. Speciation of 0.5 M DEA/4 M MDEA at 313 K. Results are shown as a fraction of total amine. Predictions made by Chakravarty[32] using the model of Austgen.[17]

higher than PZ until a loading of 0.5 while the carbamate and protonated DEA species reach their maximum around a loading of 0.6 or 0.7.

We also show a curve for PZ + $PZCOO^-$ in Figure 9. This compares the reactive amine in PZ/MDEA to DEA/MDEA. We see that the total reactive amine in the PZ blend is comparable to the DEA blend. From a kinetics point of view, the advantage of the PZ system is that its rate constant is much higher than those of DEA or MEA. Comparing the effect of temperature on carbamate stability in Figure 8, we see that the dicarbamate concentration is much lower at 343 K than at 313 K.

Figure 10 shows activity coefficients of species at 313 K in 0.6 M PZ/4 M MDEA. Volatility estimates of PZ in PZ-activated MDEA solutions are presented in Figure 11. Because total pressures and gas-phase compositions vary widely in industrial absorbers, results are presented as the vapor-side fugacity of PZ. Because the gas leaving the absorber will last be in contact with the lean amine solution entering the top of the column, all of the calculations are done at a lean loading of 0.01. PZ is seen to be very volatile as compared to MDEA and other promoters. Although the vapor pressure of PZ is comparable to MEA, the activity coefficient at infinite dilution in water is a little bit higher. At 40 °C in 0.6 M

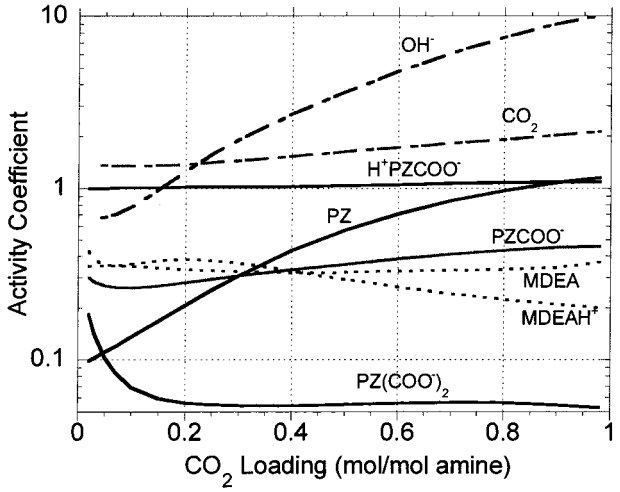

Figure 10. Activity coefficients for 0.6 M PZ/4 M MDEA at 313 K.

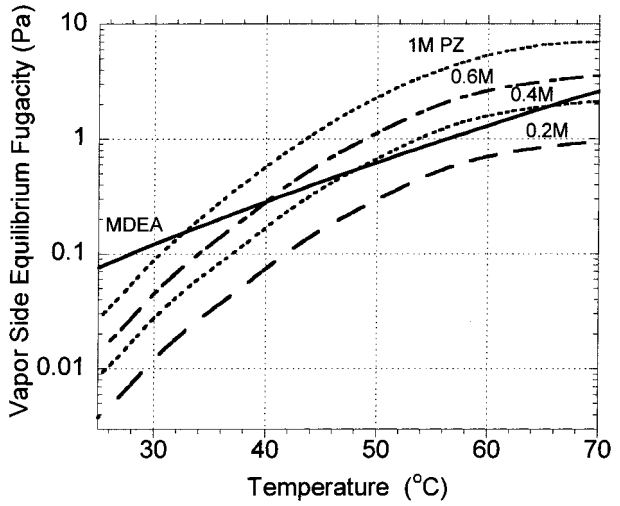

Figure 11. Prediction of PZ volatility in 4 M MDEA and various PZ concentrations. All calculations are performed at a lean loading of 0.01 mol of CO_2/mol of amine.

PZ/4 M MDEA (5 wt % of PZ/45 wt % of MDEA), PZ losses are seen to be as large as MDEA losses, even though the MDEA concentration is higher by a factor of 7.

Conclusions

The experimental solubility of CO_2 and model predictions presented in this work suggest that PZ-activated MDEA blends offer a lower equilibrium partial pressure of CO_2 at low loading than DEA/MDEA blends. Partial pressures at low loading are, however, seen to be higher than those in MEA-promoted MDEA. This is due to the carbamate stability of each of these promoters.

The most prevalent reaction product at low loading (<0.2 at low loading) is PZ carbamate. At higher loading, however, most of the PZ is seen to be in the form of protonated PZ carbamate.

The existence of the protonated carbamate and the dicarbamate have the adverse effect of stabilizing the overall carbamate formation. This leads to a higher partial pressure than that observed in MDEA at loadings above 0.3 at 313 K.

The volatility of PZ is higher than that of other promoters, and losses of PZ may be as high at those of MDEA in industrially significant concentrations. Measurements of PZ volatility in H_2O and MDEA solutions will enhance the prediction of equilibrium CO_2 partial pressure and speciation in PZ-activated MDEA blends.

NMR has proven to be a useful technique in stabilizing carbamate species and quantifying their equilibrium constants.

Our model and data show that PZ only has a large effect on solubility when the ratio of total carbon dioxide to PZ is less than 1. The model presented in this work predicts the data of other investigators at high loading as well.

PZ carbamate, dicarbamate, and protonated carbamate have been detected in significant concentrations using ^1H and ^{13}C NMR.

Literature Cited

(1) Wammes, W.; Meissner, H.; Hefner, W. Activated MDEA Process: A Flexible Process for Acid Gas Removal from Natural Gas, 73rd Annual GPA Convention, New Orleans, LA, March 7−9, 1994; Gas Processors Association: Tulsa, OK; conference preprint.

(2) Austgen, D. M.; Rochelle, G. T.; Chen, C. C. A Model of Vapor−Liquid Equilibria for Aqueous Acid Gas-Alkanolamine Systems Using the Electrolyte-NRTL Equation. *Ind. Eng. Chem. Res.* **1989**, *28* (7), 1060.

(3) Posey, M. L. Thermodynamic Model for Acid Gas Loaded Aqueous Alkanolamine Solutions. Ph.D. Dissertation, The University of Texas, Austin, TX, 1996.

(4) Pacheco, M. A.; Kaganoi, S.; Rochelle, G. T. CO_2 Absorption into Aqueous Mixtures of Diglycolamine and Methyldiethanolamine. *Chem. Eng. Sci.* **2000**, *55*, 5125−5140.

(5) Glasscock, D. A.; Critchfield, J. E.; Rochelle, G. T. CO_2 Absorption/Desorption in Mixtures of Methyldiethanolamine with Monoethanolamine and Diethanolamine. *Chem. Eng. Sci.* **1991**, *46*, 2829−2845.

(6) Critchfield, J. E. CO_2 Absorption/Desorption in Methyldiethanolamine Solutions Promoted With Monoethanolamine and Diethanolamine: Mass Transfer and Reaction Kinetics. Ph.D. Dissertation, The University of Texas, Austin, TX, 1988.

(7) Littel, R. J.; Versteeg, G. F.; Van Swaaij, W. P. M. Kinetics of CO_2 with Primary and Secondary Amines in Aqueous Solutions. II. Influence of Temperature on Zwitterion Formation and Deprotonation Rates. *Chem. Eng. Sci.* **1992**, *47*, 2037−2045.

(8) Rinker, E. B.; Ashour, S. S.; Sandall, O. C. *Acid Gas Treating with Aqueous Alkanolamines: Parts I, II, and III*; GRI/GPA Research Report RR-158. GPA Project 911, GRI Contract No. 5092-260-2345; Gas Processors Association: Tulsa, OK, 1997.

(9) Bishnoi, S.; Rochelle, G. T. Absorption of Carbon Dioxide into Aqueous Piperazine: Reaction Kinetics, Solubility and Mass Transfer. *Chem. Eng. Sci.* **2000**, *55*, 5531−5543.

(10) Bishnoi, S.; Rochelle, G. T. Physical and Chemical Solubility of Carbon Dioxide in Aqueous Methyldiethanolamine. *Fluid Phase Equilib.* **2000**, *168*, 241−258.

(11) Posey, M. L.; Rochelle, G. T. A Thermodynamic Model of Methyldiethanolamine−CO_2−H_2S−Water. *Ind. Eng. Chem. Res.* **1997**, *36*, 3944−3958.

(12) Xu, G.-W.; Zhang, C.-F.; Qin, S.-J.; Gao, W.-H.; Liu, H.-B. Gas−Liquid Equilibrium in a CO_2−MDEA−H_2O System and the Effect of Piperazine on It. *Ind. Eng. Chem. Res.* **1998**, *37*, 1473−1477.

(13) Liu, H.-B.; Zhang, C.-F.; Xu, G.-W. A Study on Equilibrium Solubility for Carbon Dioxide in Methyldiethanolamine−Piperazine−Water Solution. *Ind. Eng. Chem. Res.* **1999**, *38*, 4032.

(14) Gmehling, J.; Li, J.; Schiller, M. A Modified UNIFAC Model. 2. Present Parameter Matrix and Results for Different Thermodynamic Properties. *Ind. Eng. Chem. Res.* **1993**, *32*, 178−193.

(15) Wilson, H. L.; Wilding, W. V. Vapor−Liquid and Liquid−Liquid Equilibrium Measurements on Twenty-Two Binary Mixtures in DIPPR; Data Series No. 2; AIChE: New York, 1994; pp 63-115.

(16) Schwarzenbach, D. Structure of Piperazine Hexahydrate. *J. Chem. Phys.* **1968**, *48*, 4134−4140.

(17) Austgen, D. M. A Model for Vapor−Liquid Equilibrium for Acid gas−Alkanolamine−Water Systems. Ph.D. Dissertation, The University of Texas at Austin, Austin, TX, 1989.

(18) Smith, W. R.; Missen, R. W. Strategies for Solving The Chemical Equilibrium Problem and an Efficient Microcomputer Based Algorithm. *Can. J. Chem. Eng.* **1988**, *66*, 591.

(19) Soave, G. Equilibrium Constants from a Modified Redlich-Kwong Equation of State. *Chem. Eng. Sci.* **1972**, *27*, 1197.

(20) Chen, C. C.; Britt, H. I.; Boston, J. F.; Evans, L. B. Local Composition Model for Excess Gibbs Energy of Electrolyte Systems, Part I: Single Solvent, Single Completely Dissociated Electrolyte. *AIChE J.* **1982**, *28*, 588−596.

(21) Chen, C. C.; Evans, L. B. A Local Composition Model for the Excess Gibbs Energy of Aqueous Electrolyte Systems. *AIChE J.* **1986**, *32*, 444−454.

(22) Mock, B.; Evans, L. B.; Chen, C. C. Thermodynamic Representation of Phase Equilibria of Mixed-Solvent Electrolyte Systems. *AIChE J.* **1986**, *32*, 1655−1664.

(23) Rowley, P. L.; Wilding, W. V.; Oscarson, J. L.; Adams, M. E.; Marshall, T. L. Physical and Thermodynamic Properties of Pure Chemicals: Evaluated Process Design Data; Part 3, DIPPR; AIChE: New York, 1999.

(24) Chen, C. C.; Britt, H. I.; Boston, J. F.; Evans, L. B. Extension and Application of the Pitzer Equation for Vapor−Liquid Equilibrium of Aqueous Electrolyte Systems with Molecular Solutes. *AIChE J.* **1979**, *25* (5), 820.

(25) Brelvi, S. W.; O'Connell, J. P. Corresponding States Correlations for Liquid Compressibility and Partial Molal Volumes of Gases at Infinite Dilution in Liquids. *AIChE J.* **1972**, *18* (6), 1239−1242.

(26) Stephenson, R. M.; Malanowski, S. *Handbook of the Thermodynamics of Organic Compounds*; Elsevier Science Publishing Co.: New York, 1987.

(27) Caracotsios, M. Model Parametric Sensitivity Analysis and Nonlinear Parameter Estimation. Theory and Applications. Ph.D. Dissertation, The University of Wisconsin, Madison, WI, 1986.

(28) Bishnoi, S. Carbon Dioxide Absorption and Solution Equilibrium in Piperazine Activated Methyldiethanolamine. Ph.D. Dissertation, The University of Texas at Austin, Austin, TX, 2000.

(29) Jou, F. Y.; Mather, A. E.; Otto, F. D. Solubility of H_2S and CO_2 in Aqueous Methyldiethanolamine Solutions. *Ind. Eng. Chem. Process Des. Dev.* **1982**, *21*, 539−544.

(30) Dohnal, V.; Roux, A. H.; Hynek, V. Limiting Partial Molar Excess Enthalpies by Flow Calorimetry: Some Organic Solvents in Water. *J. Solution Chem.* **1994**, *23*, 889−900.

(31) Pagano, J. M.; Goldberg, D. E.; Fernelius, W. C. A Thermodynamic Study of Homopiperazine, Piperazine, and *N*−(2-Aminoethyl)-Piperazine and Their Complexes with Copper(II) Ion. *J. Phys. Chem.* **1961**, *65*, 1062.

(32) Chakravarty, S. Absorption of Carbon Dioxide in Aqueous Blends of Diethanolamine and Methyldiethanolamine, M.S. Thesis, University of Texas at Austin, Austin, TX, 1992.

Received for review April 9, 2001
Revised manuscript received November 9, 2001
Accepted November 13, 2001

IE0103106